

Interseismic strain accumulation in south central Chile from GPS measurements, 1996–1999

J. C. Ruegg,¹ J. Campos,² R. Madariaga,³ E. Kausel,² J. B. de Chabaliér,¹
R. Armijo,¹ D. Dimitrov,⁴ I. Georgiev,⁴ and S. Barrientos²

Received 11 May 2001; revised 24 September 2001; accepted 25 October 2001; published 8 June 2002.

[1] Two campaigns of Global Positioning System (GPS) measurements were carried out in the Concepción-Constitución area of Chile in 1996 and 1999. It is very likely that this area is a mature seismic gap, since no subduction earthquake has occurred there since 1835. In 1996, 32 sites were occupied in the range 35°S–37°S, between the Pacific coast of Chile and the Andes near the Chile-Argentina border. In 1999, the network was extended by the installation of 9 new points in the Arauco region whereas 13 points among the 1996 stations were reoccupied. The analysis of this campaign data set, together with the data recorded at eight continuous GPS sites (mostly IGS stations) in South America and surrounding regions, indicates a velocity of about 40 ± 10 mm/yr in the direction N80–90°S for the coastal sites with respect to stable cratonic South America. This velocity decreases to about 20–25 mm/yr towards the Andes. We interpret this result as reflecting interseismic strain accumulation above the Nazca-South America subduction zone, due to a locked thrust zone extending down to about 60 km depth. **INDEX TERMS:** 1242 Geodesy and Gravity: Seismic deformations (7205); 1208 Geodesy and Gravity: Crustal movements–intraplate (8110); 7230 Seismology: Seismicity and seismotectonics

1. Introduction

[2] The coastal ranges of Chile are among the most seismically active zones in the world. On average, one major earthquake of magnitude 8 has occurred every 10 years in historical times, and most of the individual broken segments of the coastal ranges have been the site of at least one magnitude 8 during the last 130 years.

[3] The south of Central Chile region, between 35°S and 37°S, experienced its last largest subduction earthquake on February 1835 [Darwin, 1851] with an estimated magnitude close to 8.5 [Lomnitz, 1971; Beck *et al.*, 1998]. This area lies immediately to the north of the rupture zone associated with the great 1960 earthquake, of magnitude 9.5 [Plafker and Savage, 1970; Cifuentes, 1989]. Part of the region from 35°S to 37°S, was damaged by the Chillan earthquake on January 25, 1939 for which the magnitude was estimated at 7.9. Recent studies demonstrated that this event was not a typical subduction earthquake, but was a slab-pull event due to the release of tensional stresses within the downgoing slab [Campos and Kausel, 1990; Beck *et al.*, 1998]. Further North, the Talca earthquake of December 1, 1928, was interpreted as a shallow dipping thrust event, [Lomnitz, 1971; Beck *et al.*, 1998]. Despite the uncertainties that remain on the impor-

tance of the 1928 and 1939 earthquakes with respect to the seismic cycle, the region from 35°S–37°S is a likely spot for a major subduction earthquake in the coming decades.

[4] The seismicity of the region remained largely unknown and imprecise because of the lack of a dense seismic network. What is the potential for a future earthquake? How is the current plate motion accommodated by crustal strain in this area? With the aim to resolve these questions, a seismic field experiment was carried out in 1996 in the Concepción-Constitución area in the framework of a Chilean-French project. The results of this experiment reveal the distribution of the current seismicity, focal mechanism solutions, and geometry of the subduction [Campos *et al.*, 2001]. As a second experiment inside this project, the GPS network was initiated in 1996 in order to study the crustal deformation and place it in the tectonic framework of global plate motion.

[5] In this paper we present the GPS measurements of 1996 and 1999, and we estimate for the first time the interseismic velocity at 13 points above the subduction of the Nazca plate beneath South America. This data set provides a direct measurement of the velocity gradient that shows shortening between the Pacific coast and the Andean belt. We interpret it as interseismic strain accumulation.

2. GPS Measurements and Data Processing

[6] GPS measurements in the Concepción-Constitución area began in December 1996 with the installation and first observation of 32 sites in 3 transects (Figure 1). We set up a 13 site N-S transect along the Pacific coast between the Maule river and the city of Concepción (PTU, CO1-CO9, CBQ, CML, MLA, UCO); a northern W-E transect of 8 sites between Constitución on the Pacific coast and the Chile-Argentina border (CO1, CT2, CT3, CT4, COLB, CT6, CT7, CT8); another W-E transect of 6 sites from the Arauco peninsula, south of Concepción and the Laja lake near the Chile-Argentina border (with two sites in the coastal zone: RMN, LTA, and 4 sites between the foothills of the Andes and the Argentina border: MRC, MIR, CLP, LLA). Five additional points were installed in the Central Valley (BAT, PUN, QLA, CHL, NIN). During this first experiment we used 9 Ashtech Z12 and 3 Trimble SSE receivers, all sampling every 30 seconds. Used antennas were from type 1 and type 2. Each site was surveyed 20–30 hours in average for 2 or 3 days of measurement. Three stations (QLA, COLB, CO6) operated continuously during the 6 days of the campaign.

[7] The network was partially remeasured and extended in March 1999. Nine new sites were installed and observed on the southern part of the 1996 network in order to complete the Arauco-Laja lake profile (LLI, RAQ, CAP, PUL, LAJ, SLT, GUA, SGE and TET) and 13 sites were remeasured during the 1999 campaign (Figure 1). Among them, the sites QLA, UCO, PUN and CO6 were observed continuously during more than 96 hours. We used 7 Ashtech Z-12 receivers, sampling every 30 seconds, equipped with choke-ring antennas.

[8] To analyse the GPS data, we follow the now standard procedures described by Feigl *et al.* [1993] and Calais *et al.* [1998] using an updated version (9.94) of the GAMIT software package [King and Bock, 1998], followed by a GLOBK analysis [Herring *et al.*, 1998].

¹Institut de Physique du Globe, Paris, France.

²Universidad de Chile, Santiago, Chile.

³Ecole Normale Supérieure, Paris, France.

⁴Bulgarian Academy of Sciences, Sofia, Bulgaria.

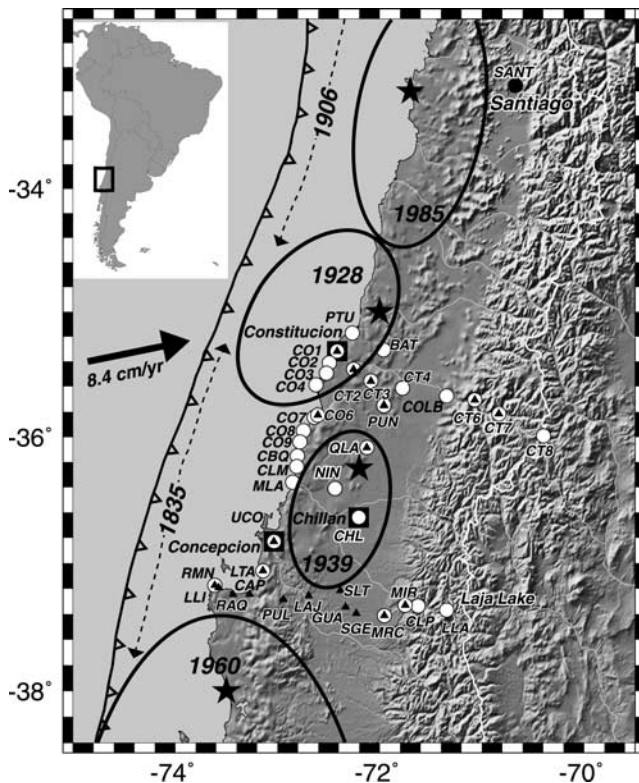


Figure 1. Location of GPS stations. Open circles are stations occupied in December 1996, triangles in 1999. Large ellipses and black stars indicate respectively rupture zones and epicenters of the 1928, 1939 and 1985 earthquakes [Campos *et al.*, 2001]. Approximate extension of 1835 and 1960 earthquake ruptures are shown by dashed lines. Squares indicate the main cities. Inset shows location of studied area. Plate convergence (8.4 cm/yr) from De Mets *et al.* [1990].

[9] We calculated daily solutions in which we estimated station coordinates, satellite state vectors, 7 tropospheric zenith delay parameters and phase ambiguities using double difference phase measurements. We applied azimuth and elevation dependant antenna phase center models. Six IGS stations operating in the neighbouring of South America (AREQ, BRAZ, EISL, FORT, LPGS, SANT) were included in the processing to serve as ties with the International Terrestrial Reference Frame ITRF97 [Boucher *et al.*, 1999], and additionally we included also in the processing our permanent station (UAP0) operating in Northern Chile. We used IGS final orbits, IERS earth rotation parameters, and applied IGS tables for azimuth and elevation corrections of the antenna phase center. In a second step, the least square adjustment vectors and their corresponding variance-covariance matrix for station positions and other parameters obtained for each daily GAMIT solutions were combined using the GLOBK software [Herring *et al.*, 1998] to estimate the station positions and velocities.

3. Velocity Solution

[10] We first defined the reference frame by constraining the positions and velocities of 4 IGS stations in stable South American (KOUR, FORT, BRAZ and LPGS) to their known ITRF97 values [Boucher *et al.*, 1999]. In our GLOBK adjustment, the fiducial stations are constrained to 1 cm for North and East coordinates, and 3 cm for elevation; 1 mm/yr for North and East velocities and 10 mm/yr for up velocity. The other stations are loosened to 5 m in position and 25 cm/yr in velocity.

[11] Obtained velocities in the ITRF97 are shown in the left part of Table 1. While the aim of this paper is not to estimate a geodetic motion of the SOAM plate but to determine the strain accumulation at the regions bordering the subduction zone, we obtained the site velocities with respect to the stable part of South America by subtracting to our ITRF estimation the motion predicted at each station by the Nuvel-1A no-net rotation model [Argus and Gordon, 1991].

[12] The data were also processed separately using the Bernese software [Rothacher and Mervart, 1996], by two of us (D. Dimitrov and I. Georgiev). The solution differs at the level of 2–5 mm/yr, which remains within the 95% confidence ellipses. The internal deformation pattern is very similar, particularly the east-west gradient of the horizontal velocity.

[13] Figure 2 maps the GAMIT/GLOBK velocity field in the stable South America reference frame. The observed velocity decreases strongly (Figure 3a) from the coast of Chile to the interior of South America (here limited to the border Chile-Argentina). The coastal points show relative velocities in the range of 40–50 mm/yr, whereas the points located in the foothills of the Andes Cordillera move more slowly at 18–25 mm/yr like the IGS station SANT.

[14] The average direction of all velocity vectors (relative to SOAM craton) falls in the range $75^\circ \pm 8$, within few degrees of the relative plate convergence (Figure 2). The relative plate velocity between Nazca and stable SOAM plates, estimated along the Chilean coast from current plate motion models [Argus and Gordon, 1991] is in the range 79–83 mm/yr (respectively at 20°S and 38°S), with a mean convergence direction of about 76°N .

4. Discussion

[15] The southern profile, between the Arauco peninsula (RMN) and the Andes area (LLA) is particularly interesting. The nearest point to the trench, RMN, located at the westernmost end

Table 1. Velocity Vectors of the GPS Stations Used in this Study

Site	Lon	Lat	Our estimation				SOAM	
			vE	vN	sE	sN	vE	vN
1	2	3	4	5	6	7	8	9
Continuous stations (IGS in South America)								
BRAZ	-47.88	-15.95	-5.6	7.6	1.0	1.0	-1.0	-4.7
FORT	-38.43	-3.88	-4.2	10.1	0.9	0.9	2.4	-2.3
KOUR	-52.81	5.25	-3.3	9.8	0.9	0.9	2.6	-1.6
LPGS	-57.93	-34.91	-3.1	7.6	0.9	0.8	-2.7	-2.6
AREQ	-71.49	-16.47	11.1	11.6	0.9	0.9	12.4	0.5
SANT	-76.67	-33.15	17.7	13.8	0.8	0.7	15.5	3.2
OHIG	-57.90	-63.32	15.2	9.1	1.0	1.0	11.8	-3.0
EISL	-109.4	-27.15	68.0	-9.3	1.0	0.9	66.5	-11.
South central Chile local network								
UAP	-70.14	-20.24	19.2	12.6	1.8	1.0	22.4	1.1
CO1	-72.41	-35.32	32.2	19.6	2.6	1.1	46.2	6.3
CO6	-72.61	-35.83	32.9	17.9	1.6	0.9	28.1	8.2
CT2	-72.25	-35.46	36.7	18.5	3.1	1.3	42.7	7.0
CT3	-72.09	-35.56	36.3	20.4	2.8	1.3	37.2	12.7
CT6	-71.07	-35.71	23.8	16.7	1.7	0.9	28.1	7.1
CT7	-70.83	-35.81	18.6	14.2	2.7	1.1	23.0	3.4
LTA	-73.14	-37.06	22.2	20.8	5.9	2.0	55.9	9.4
MIR	-71.75	-37.33	13.9	13.6	2.2	1.2	-2.2	1.7
MRC	-71.95	-37.41	20.8	13.7	1.8	1.1	7.0	2.0
PUN	-71.96	-35.75	28.1	15.5	1.6	0.9	20.9	5.0
QLA	-72.12	-36.08	29.7	18.5	1.4	0.9	28.1	8.8
RMN	-73.61	-37.18	43.4	22.0	2.6	1.4	58.6	19.3
UCO	-73.03	-36.83	32.5	22.1	1.9	1.1	29.1	12.4

Site Id. and location (in $^\circ$) of GPS points (1–3). East and North Velocities with respect to the ITRF97 (4–5) and associated formal errors (6–7) in mm/yr (one standard deviation). Velocities estimated with respect to the stable South America (8–9).

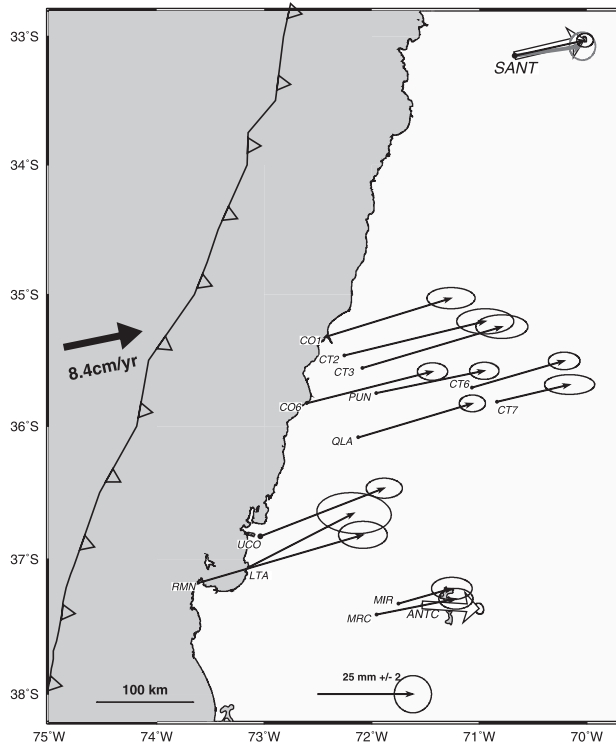


Figure 2. GPS-derived velocities relative to stable South America for the 13 sites of the survey measured in the two epochs (1996 and 1999). Large open vectors are from *Bevis et al.* [1999] for the sites of SANT (IGS station) and ANTC (Antuco). The velocity of SANT from *Angermann et al.* [1999] is also show (in bold grey).

of the Arauco peninsula shows a velocity of about 48 ± 10 mm/yr, whereas the points near the Andes, MRC, MIR (but also CT7, SANT), shows velocities of about 20 ± 5 mm/yr.

[16] The Arauco peninsula is a rise on the oceanic part of the subduction zone with respect to the mean coastal line. It shows evidences of both quaternary and contemporary uplift. Indeed *Darwin* [1851] reported 3 m of uplift at Santa Maria island located 10 km north of the Arauco Peninsula (RMN station, Figure 2) due to the 1835 earthquake. On the other hand, this area constitutes the limit between the rupture zones of the 1835 and 1960 earthquakes. As such, it might play an important role in the segmentation of the subducting slab. In order to study this particular tectonic context we densified the geodetic network in 1999 by installing nine new points between the Andes mountains and the Arauco peninsula.

[17] This tectonic situation is similar to that of the Mejillones Peninsula which seems to have acted as a limit to southward propagation for the 1877 large earthquake in Northern Chile, and to northward propagation during the 1995 Antofagasta earthquake [*Armijo and Thiele, 1990; Ruegg et al., 1996*].

[18] We may now compare our velocity estimate with previously published values [*Angermann et al., 1999; Bevis et al., 1999*] for two stations in the area (IGS station SANT, and ANTC located near the south-eastern end of our study).

[19] For SANT, our solution in a stable SOAM reference frame gives a velocity of 18.93 ± 1.2 mm/yr, very close to the *Bevis et al.* [1999] velocity 18.92 ± 0.04 mm/yr, both oriented $N77^\circ$ very close to the convergence direction given by the plate motion. *Angermann et al.* [1999] found a velocity of about 17.97 ± 1.5 mm/yr, oriented $N82^\circ$. The slight discrepancy can be due to a misalignment between the reference frame and/or the pole used by each author.

[20] The ANTC site used by *Bevis et al.* [1999] is located 26 km East of our MIR station. The *Bevis et al.* [1999] estimation for the ANTC velocity is 15.01 ± 0.76 mm/yr with a direction $N93^\circ$, while for our nearest point MIR we found a velocity of about 14.59 ± 2.50 mm/yr with a direction of $N73^\circ$ (very similar to the convergence direction).

5. Modelling the Interseismic Deformation

[21] To model the interseismic behaviour, we first defined the geometry of the subduction contact, taking into account the distribution of earthquakes along a cross section recorded during the 1996 seismic field experiment [*Campos et al., 2001*]. The mean orientation of both trench and coast is $N19^\circ E$ so that a vector perpendicular to the trench points in the direction $N109^\circ$, whereas the mean convergence direction is about $N76^\circ$. In the upper part of the subduction interface, a “seismically coupled zone” is defined as the portion of the plate interface that is capable of producing a thrust earthquake. This zone extends from the trench to a depth of about 35–50 km [*Oleskevich et al., 1999*]. In order to closely follow the trend of the seismicity [*Campos et al., 2001*] we shape the interface to be convex upwards as sketched Figure 3b. During the interseismic stage, we assume this zone to be locked.

[22] The conventional back-slip model is commonly used by most authors to account for the interseismic deformation at subduction zones [*Savage et al., 1983*]. Used in the case of a curved interface in the coupling zone this approach may lead to biased results as discussed by *Vergne et al.* [2001].

[23] We consider a reverse slip imposed on the deeper part of the plate interface, ie on the down-dip extension of the locked fault, that simulates the ductile shear zone in depth.

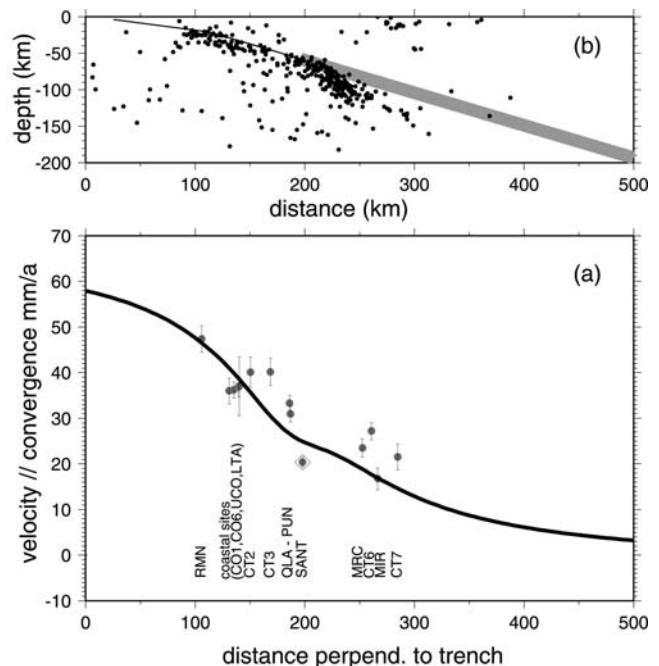


Figure 3. (a) Cross section of observed (grey dots) and modeled (curve) deformation. Horizontal velocities parallel to the plate convergence $N76^\circ$ are projected in the direction $N109^\circ$, perpendicular to the trench direction between latitudes $34^\circ N$ – $38^\circ N$. (b) Cross section perpendicular to the trench showing the “seismically coupled zone” (black line) and the “steady-slip” model where reverse slip is imposed (thick grey line). The dots are hypocenter determined during the 1996 experiment [*Campos et al., 2001*].

[24] A cross section of the model is given in Figure 3b, with the geometry of the “seismically coupled zone” (thin black line) and the “reverse steady-slip” model (red thick line) for the deeper part of the plate interface. We use the formalism developed by Okada [1985] combining a set of dislocations embedded in an elastic half space. We impose a 84 mm/yr velocity vector, consistent with the plate convergence [DeMets *et al.*, 1990] along all the deeper part of the dislocation with a rake of about 120°.

[25] This approach requires a dislocation that extends from h_c , the coupling depth, to infinite in depth and along the strike direction to reduce the side effect of the dislocation in the studied area. When this model produces a residual deformation in the far field, we subtract from our modeled values the motion calculated at a point away on the craton in order to compare with our observed velocity vectors relative to stable South America.

[26] The “seismically coupled zone” being locked, its geometry has no effect on the modeled deformation.

[27] We tried a coupling depth h_c in the range 29–70 km. The best fit with observations yields $h_c = 58$ km consistent with the thermal model developed by Oleskevich *et al.* [1999]. The observed and calculated velocities (component parallel to the plate convergence N76°) projected along a N109° line, perpendicular to the strike, are shown on Figure 3a.

[28] As a consequence of this model, the area located at a distance of 400 km from the trench, (300 km from coast and very close to the Chile Argentina border) shows (Figure 3) a calculated velocity lower than 5 mm/yr. So the accumulation of deformation is limited to the coastal area and the Andes, and the area further east can be considered as belonging to quasi stable SOAM.

6. Conclusions

[29] A GPS geodetic network, including 41 stations, was installed in south central Chile subduction zone between 1996 and 1999 in order to monitor the deformation associated with the seismic cycle in a region which we believe is the likely site of a large earthquake in the future. During the first experiment in 1996, 32 stations following 3 transects were set up in the region extending between 35°S (Constitución) and 37°S (Concepción). In 1999 we densified the southern profile between the Arauco peninsula and the foothills of the Andes mountains, with 9 new points, while 13 of the 1996 stations were remeasured.

[30] The analysis of this GPS data set, together with data from eight continuous GPS sites in South America and surrounding regions, shows velocities in the 45–18 mm/yr range for the GPS sites with respect to stable South America. The mean direction of the velocity vector falls in the range N74° ±5 for most of them, which is approximately the convergence direction of the Nazca plate with respect to the SOAM plate. The magnitude of the velocity vectors decreases rapidly from the coast towards the Andes. We interpreted this deformation pattern as elastic deformation with a model in which the plate interface is locked down to 60 km and freely slipping at deeper depths.

[31] This strong decrease of the GPS vectors in south central Chile region reflects the interseismic strain accumulation above the Nazca-South America subduction zone, in an area which is probably mature for a next large earthquake because it does not experienced a large subduction earthquake since 1835.

[32] **Acknowledgments.** This work is part of a cooperative project between Universidad de Chile, Santiago, Institut de Physique du Globe de Paris and Ecole Normale Supérieure, Paris. It was supported by a European Community contract C11-CT94-0109 and Project ECOS/CONICYT contracts C98U2 and C97U01. The GPS group at MIT, Tom Herring, Bob King, Simon McClusky graciously provided software, files and advice. All

figures were made with the public domain software GMT [Wessel and Smith, 1998]. We thank all participants in the field works, and among them E. Clevede, T. Monfret, L. Hernandez, R. Fromm, R. Rauld. We are grateful to Kurt Feigl and anonymous reviewers for helpful suggestions and improvement of the manuscript. Contribution IPGP No 1794.

References

- Angermann, D., J. Klotz, and C. Reigber, Space geodetic estimation of the Nazca-South America Euler vector, *Earth Planet. Sci. Lett.*, *171*, 329–334, 1999.
- Argus, D. F., and R. G. Gordon, No-net rotation model of current plate velocities incorporating plate motion model NUVEL-1A, *Geophys. Res. Lett.*, *18*, 2039–2042, 1991.
- Armijo, R., and R. Thiele, Active faulting in Northern Chile: Ramp stacking and lateral decoupling along a subduction plate boundary, *Earth Planet Sci. Lett.*, *98*, 40–61, 1990.
- Beck, S., et al., Source characteristics of historic earthquakes along the central Chile subduction zone, *J. South. American Earth Sci.*, *11*, 115–129, 1998.
- Bevis, M., et al., Crustal motion North and South of the Arica deflection: comparing recent geodetic results from Central Andes, *Geochem. Geophys. Geosyst.*, vol. 1, 1999.
- Boucher, C., Z. Altamimi, and P. Sillard, The 1997 International Terrestrial Reference Frame (ITRF97), *I.E.R.S. Technical note 27*, 1999.
- Calais, et al., Crustal deformation in the Baikal rift from GPS measurements, *Geophys. Res. Lett.*, *25*(no 21), 4003–4006, 1998.
- Campos, J., and E. Kausel, The large 1939 Intraplate earthquake of Southern Chile, *Seis. Res. Lett.*, *61*, 1990.
- Campos, J., D. Hatzfeld, R. Madariaga, E. Kausel, G. Lopez, A. Zollo, R. Fromm, G. Iannaccone, and S. Barrientos, A seismological study of the 1835 seismic gap in South Central Chile, *Earth Planet Sci. Lett.*, (in press), 2001.
- Cifuentes, I. L., The 1960 Chilean earthquake, *J. Geophys. Res.*, *94*, 665–680, 1989.
- Darwin, C., Geological observation on coral reefs, volcanic island and on South America, 768 pp., Londres, 1851.
- DeMets, C., et al., Current plate motions, *Geophys. J. Int.*, *101*, 425–478, 1990.
- Feigl, et al., Space geodetic measurements of crustal deformation in Central and Southern California, 1984–1992, *J. Geophys. Res.*, *98*, 21,677–21,712, 1993.
- Herring, T., Documentation for GLOBK: Global Kalman filter for VLBI and GPS analysis program, version 4.1, MIT, 1998.
- King, R., and Y. Bock, Documentation for the GAMIT GPS analysis software, version 9.7, MIT, 1998.
- Lomnitz, C., Grandes terremotos y tsunamis en Chile durante el periodo 1535–1955, *Geofis. Panamericana*, *1*, 151–178, 1971.
- Okada, Y., Surface deformation to shear and tensile faults in a half space, *Bull. Seism. Assoc. Amer.*, *75*, 1135–1154, 1985.
- Oleskevich, D. A., R. D. Hyndman, and K. Wang, The updip and downdip limits to great subduction earthquakes: Thermal and structural models of Cascadia, SW Japan and Chile, *J. Geophys. Res.*, *104*, 14,965–14,991, 1999.
- Plafker, G., and J. C. Savage, Mechanism of the Chilean earthquake of May 21 and 22, 1960, *Geol. Soc. Am. Bull.*, *81*, 1001–1030, 1970.
- Rothacher, and Mervart, BERNSE GPS software version 4.0, Astronomical Institute University of Berne, 1996.
- Ruegg, et al., The Mw = 8.1 Antofagasta earthquake of July 30, 1995: First results from teleseismic and geodetic data, *Geophys. Res. Letters*, *23*(9), 917–920, 1996.
- Vergne, J., R. Cattin, and J. P. Avouac, On the use of dislocations to model interseismic strain and strain build-up at intercontinental thrust faults, *Geophys. J. Int.*, *147*, 155–162, 2001.
- J. C. Ruegg, J. B. de Chabaliere, and R. Armijo, CNRS, UMR 7580 & 7578, Institut de Physique du Globe, Paris, France, 4, place Jussieu, 75252 Paris cedex 05, France. (ruegg@ipgp.jussieu.fr)
- S. Barrientos, J. Campos, and E. Kausel, Universidad de Chile, Departamento de Geofísica, Santiago, Chile. (jaime@dgf.uchile.cl)
- R. Madariaga, CNRS, UMR 8538, Ecole Normale Supérieure, Paris, France.
- D. Dimitrov and I. Georgiev, Bulgaria Academy of Sciences, Institut of Geodesia, Sofia, Bulgaria.